Cell-free production of full-length ice nucleating protein InaZ

Irina V. Novikova[1], Swarup China[1] & James E. Evans[1,2,*]

Affiliations:

1) Environmental Molecular Sciences Laboratory, Pacific Northwest National Laboratory, 3335 Innovation Blvd., Richland, WA 99354, USA
2) School of Biological Sciences, Washington State University, Pullman, WA 99164, USA

Corresponding Author(s): james.evans@pnnl.gov

Abstract

Unlike inorganic or other synthetic alternatives, ice nucleating proteins - INPs - remain the most efficient ice nuclei today. Their potential applications in cryo-preservation, biomedicine, food industry and in the modulation of climate are widespread. Nevertheless, due to multiple difficulties to express these proteins in full-length in necessary yields using cell-based recombinant methods, further applications are limited. As a result, our understanding of the structure and ice nucleation mechanism for this class of proteins is also incomplete. Using wheat-germ cell-free expression pipeline, we successfully expressed and purified full-length ice nucleating protein InaZ from *Pseudomonas syringae*, known as a model INP. High protein yield and solubility has been achieved using this cell-free platform, allowing us to confirm the heterogeneous nature of InaZ assembly using negative stain TEM. The cell-free produced InaZ protein was confirmed to be functional by conducting ice nucleation experiments inside a dynamic environmental scanning electron microscope (ESEM). We believe that the current platform will be suitable for expressing other INPs of interest and can be further employed for industrial and structural characterization needs as INP source.

Keywords
Ice nucleating proteins, INPs, InaZ, ice nucleation, cell-free protein expression, wheat germ

Introduction

Ice nucleating proteins, INPs, belong to a rare class of proteins that evolved a highly unique ability to enhance ice nucleation in the supercooled water at sub-zero temperatures. These proteins reside in the outer cell membrane of a few select ice-nucleation-active (Ina+) bacterial strains, which include *Pseudomonas* and *Erwinia* species[1,2]. The presence of such bacterial strains on leaf surfaces are known to cause significant frost injuries to plants [3,4]. Ina+ bacteria have also been widely detected in air and cloud water, suggesting key roles in the atmospheric glaciation and cloud evolution[5-8].

The most active Ina+ strain, known to date, is *Pseudomonas syringae*[1]. The first ice-nucleating protein, described at the sequence level, originated from that strain and was found to contain exactly 1,200 amino acids[9]. It was further designated as InaZ and remains the most-characterized INP today. Based on the aminoacid sequence analysis, InaZ protein body was initially divided into three main domains: N-terminal (1-175 aas), central (176-1151 aas) and C-terminal (1152-1200 aas). While N-terminal domain in INPs is responsible for anchoring to the outer membrane of the cell and transmembrane transport[10], the central and largest domain is at the core of the ice nucleation mechanism[9]. This region was found to be of the most unusual architecture with striking number of repetitive peptide blocks with three orders of periodicity. Individual 8-residue blocks (112 of them) organize in 16-residue repeats, which are a part of higher-order 48-residue arrangements. Deletion experiments of the various portions of this domain did not

pinpoint to an individual region responsible for the ice activity and rather suggested a quantitative contribution of individual repeats to the ice formation mechanism[9,11]. More recently, two aminoacid repeats, STxT and ExSxT, were identified as key ice-nucleating motifs according to computational simulations[12].

Experimental *in situ* radiation studies determined the size of active ice-nucleating structures and found that they vary significantly in sizes depending on the nucleation temperature[13]. At lower temperature range (-12 ºC to -13 ºC), the mass of active complexes was found to correspond to a single protein of 150 kDa. Upon the increase in the ice nucleation temperature, the mass of the complex increases log-linearly and achieves the maximum of 8000 kDa at -2 ºC, which corresponds roughly to a multimeric assembly of 53 InaZ proteins. Many additional experimental and modelling efforts have also shown that the multimerization of InaZ or its fragments seem to be critical for its nucleation performance[14-16]. However, questions still remain regarding the full-length structure of InaZ and the mechanism of its action.

To date, the majority of all preliminary characterization has been done on natively-purified InaZ from the cell membranes of *Pseudomonas syringae*, where quantities are generally not sufficient or pure enough for the structural work. Other cell-based recombinant expression trials on closely related INPs yielded protein in inclusion bodies when over-expressed and require additional solubilization[17,18]. Recently, successful recombinant expression of InaZ fragments from 240 up to 576 residues has been achieved in *E. coli* while the expression of longer fragments failed[19]. Using CD and IR spectroscopy, the detailed biophysical characterization of 240-residue InaZ fragment showed that, most likely, it exists as an elongated monomer and it is composed mainly of β-sheets and random coil. However, that same report mentioned that the fragment used for those studies did not display any detectable nucleation activity[19]. Thus, a new approach, which can synthesize and purify InaZ protein while simultaneously retaining its functionality, is needed in order to answer many of the open questions in the field of InaZ mechanism, structure, and kinetics. In this work, we demonstrate that, by using wheat germ cell-free protein expression technology, we can successfully express and purify InaZ recombinantly (as full-length or truncated isoform) while maintaining ice nucleation capability.

Materials and Methods

The InaZ vector construction for cell-free protein synthesis. A host plasmid containing a major portion of InaZ gene (aas 1- 1179) was obtained from addgene plasmid repository, #26759[20]. Using PCR, the gene was amplified and extended to include additional DNA sequence to encode extra 21 amino acids on its C-terminal to obtain a full-length clone and provide extra DNA regions as purification tags. PCR reactions were carried out using the Q5 Hot Start High-Fidelity 2X Master Mix from New England Biolabs. All DNA primers were purchased from Invitrogen. The template vector was pEU (pEU-MCS-TEV-HIS-C1) from CellFree Sciences. Obtained PCR products, such as linearized pEU template and the gene insert, were first gel-purified using Zymoclean Gel DNA recovery kit from Zymo Research and subjected to Gibson Assembly. The Gibson Assembly Master Mix from New England Biolabs was used as recommended. The assembled product has been used to transform an *E. Coli*, which was later plated on a carbenicillin-containing agar plate and grown at 37°C overnight. Several individual colonies were selected and grown overnight in LB medium, supplemented with carbenicillin. Plasmids were extracted using QIAGEN Plasmid Mini Kit and further sent for sequencing to MCLAB. Successful clones were later grown in larger quantities of LB broth (with carbenicillin) and harvested using the QIAGEN Plasmid Maxi kit.

Cell-free protein expression and 3XFLAG purification of InaZ proteins. Protein synthesis was carried out at MAXI-scale in a bilayer format using Wheat Germ Protein Research Kit (WEPRO7240 DTT free) from CellFree Sciences. Shortly, 25 µl of pEU plasmid (1 µg/µl) were mixed with 144 µl of water, 50 µl of 5xTranscription Buffer, 25 µl of 25 mM NTP mix, 3.125 µl of RNase inhibitor and 3.125 µl of SP6 polymerase and incubated at 37°C for 4 hours with shaking at 640 rpm on the Thermomixer C incubator from Eppendorf. Upon completion, 1 µl of the transcription mixture was loaded on the E-gel precast agarose gel (Invitrogen) to assess the mRNA integrity. Then 250 µl of transcription reaction were mixed with 250

µl of wheat germ extract (WEPRO7240 DTT free), 1.25 µl of 20 mg/ml creatine kinase and 1 µl of 1M DTT. The mixture was then transferred to the bottom of the individual well of a standard 6-well plate, prefilled with 5.5 ml of translation buffer 1x SUB-AMIX SGC supplemented with DTT up to 4 mM. To prevent evaporation, wells were sealed with Parafilm. The reaction was carried out for at least 20 hours at 15°C with no mixing at Thermomixer C from Eppendorf. The contents were then gently mixed by a pipette, transferred to a new tube and centrifuged at 20,000 g for 15 min. The supernatant fraction was then buffer-exchanged to TBS (50 mM Tris-HCl, pH 7.5, 150 mM NaCl) using pre-equilibrated in TBS 5 ml Zeba Spin Desalting Columns from Thermofisher (this step is critical to remove DTT) and further subjected to the protein purification procedure using 3XFLAG tag. The purification has been carried out using ANTI-FLAG M2 magnetic beads from Sigma in combination with Magnetic Separation Stand from Promega. For MAXI-scale protein synthesis, 800 µl of ANTI-FLAG M2 bead suspension (400 µl of packed gel) was first equilibrated in TBS buffer and then combined with the translation mixture. The binding was carried out for 1 hour at room temperature with shaking on the ThermoMixer C (~1100 rpm). Using the magnetic stand, the supernatant was removed and discarded, and the beads were then washed 3 times with TBS buffer. To elute the bound protein, TBS buffer supplemented with 150 µg/ml 3XFLAG peptide (Sigma) was applied to the beads, and the mixture was left shaking for 20 min. Then, the supernatant fraction was collected, and the elution procedure was repeated one more time. Two elution fractions were combined, concentrated to ~ 100 µl and buffer exchanged to TBS using 10 kDa amicons from EMD Millipore.

ProteoLiposome cell-free protein expression of 3XFLAG-InaZ. ProteoLiposome BD Expression Kit from CellFree Sciences has been used to express and purify full-length 3XFLAG-InaZ protein. Shortly, 13 µl of pEU 3XFLAG-InaZ plasmid (1 µg/µl) were mixed with 75 µl of water, 26 µl of 5xTranscription Buffer, 13 µl of 25 mM NTP mix, 1.62 µl of RNase inhibitor and 1.62 µl of SP6 polymerase and incubated at 37°C for 5 hours with shaking at 640 rpm on the Thermomixer C incubator from Eppendorf. The entire transcription mixture was further combined with 149 µl of 1xSUB-AMIX SGC buffer, 125 µl of WEPRO7240, 1 µl of 20 mg/ml creatine kinase and 100 µl of freshly hydrated 50 mg/ml Asolectin liposomes (provided as part of Proteoliposome kit). The solution contents were gently mixed by pipetting and transferred to the bottom of the dialysis cup, prefilled with 2 ml of 1xSUB-AMIX SGC buffer. Slide-A-Lyzer Dialysis Device (10K MWCO, 2 ml, ThermoFisher) has been used for the latter where 43 ml of 1xSUB-AMIX SGC were used as a feeding buffer. The translation reaction was carried out in this bilayer-dialysis format overnight at room temperature and in the vibration-free setting. The next day, 2.5 ml of the reaction mixture was gently mixed by pipetting, transferred to a new tube and then centrifuged for 10 min at 13,500g at 4°C. The supernatant was removed, and the pellet was washed three times with 1 ml of TBS buffer using the same centrifugation settings as above. After the final wash, 100 µl of TBS was added to the pellet in order to re-suspend the liposome-protein complexes. The final mixture was split in 10 µl aliquots, which were further flash-frozen in liquid nitrogen and stored at -80°C until future use.

SDS-PAGE electrophoresis. Protein expressions were evaluated on 10% Mini-PROTEAN TGX Precast Protein (Bio-Rad). For sample preparation, 3 µl of a protein solution was mixed with 4 µl of 500 mM DTT and 7 µl of the 2x Laemmi Sample Buffer (Bio-Rad) and then denatured at 90°C for 5 minutes, snap-cooled on ice and loaded on the gel. The general running conditions for SDS-PAGE were 1 hour at 150V in the 1X Tris-Glycine-SDS Running Buffer (Bio-Rad). The gels were further stained with Bio-Safe Coomassie Stain from Bio-Rad. For molecular size estimation and protein yield quantification purposes, Broad Range Protein Molecular Weight Markers from Promega were used.

TEM imaging. An ultrathin carbon film on lacey carbon (01824, Ted Pella) was glow discharged with the carbon side up at 10 mA for 30 seconds using PELCO easiGlow from Ted Pella. Then 3 µl of protein solution (~0.005 mg/ml) was deposited on the carbon side and let to absorb for 1 minute. The excess of solution was blotted away, and 15 µl of 2% PTA stain has been added on the top and incubation continued for additional 1 min. The excess of the stain was wicked away, and the grid was let to air-dry. Micrographs were acquired on 300kV FEI Environmental TEM.

Ice nucleation experiments using dynamic ESEM. Four samples (1 ml each) were freshly prepared right before the ice nucleation experiments: (1) 0.1xTBS buffer (5 mM Tris-HCl, pH 7.5, 15 mM NaCl, (2) 0.7 μg/ml of InaZΔN in 0.1xTBS buffer, (3) 0.1xTBS buffer supplemented with liposomes, and (4) 12 μg/ml of InaZ-liposome in 0.1xTBS buffer. Samples 1 and 3 were included as negative controls. The tests were also conducted in the low salt buffer to minimize deliquescence. Droplets were generated by nebulization of solution into a nitrogen gas stream at 3 lpm using a medical nebulizer (8900-7-50, Salter Laboratories) and deposited on silicon nitride substrate (Silson Ltd). Experiments were performed in an Environmental Scanning Electron Microscope (Quanta 3D model, FEI, Inc.), equipped with a custom-built ice nucleation platform (IN-ESEM)[21]. The IN-ESEM platform consists of a cryo-cooling stage coupled with a resistively heating element (Minco Product Inc.) and a temperature control unit (Model 22C, Cryogenic Control Systems, Inc.). To monitor the temperature of the droplets, a temperature sensor (±0.15 K, Pt-100, Omega Engineering Inc.) was mounted below the sample holder. A mixing chamber was used to combine ultra-high purity N_2 (g) from a temperature-controlled water reservoir and dry N_2 (g) to get desired dew point (T_d). Humidified N_2 (g) was then pumped into the ESEM chamber. A chilled mirror hygrometer (GE Sensing, Model 1311XR) was used to measure the T_d. Imaging was performed using a gaseous secondary electron detector.

Experiments were performed under isothermal conditions where the temperature of the substrate (droplet/particle, T_p) was kept constant at 250 K, and the partial pressure of water vapor was increased to raise the relative humidity with respect to ice - RH_{ice}. Droplets from InaZ-liposome complex were also investigated at multiple temperatures (250K, 240K, 245K, and 235K) at the same final concentration of 12 μg/ml for InaZ. The onset (first nucleation event) was monitored by slow increase in the RH_{ice}. A calibration experiment was followed after each ice nucleation event to calibrate T_p against T_d as described previously[22,23]. The RH_{ice} was calculated based on T_p and T_d measurements[22,24]. For every sample, three replicate experiments were carried out.

Results

Despite early discovery of InaZ, its experimental structure and the structures of other discovered INP today still remain unsolved and the detailed mechanism for their ice nucleation properties is incomplete. Access to full-length and functional INP has been challenging due to their large size and tendency for aggregation. Those same factors have also hindered recombinant expression and purification efforts and limited the applications of these proteins to synthetic biology approaches. Due to previous unsuccessful trials to express and purify full-length InaZ in *E. coli*[19], we decided to utilize the wheat germ cell-free expression system. It is a plasmid-based cell-free pipeline for high yield synthesis of proteins up to 200 kDa, which displays high solubility rates and quick turnarounds[25,26].

During our cloning efforts to transfer the InaZ gene from the host vector to our desired plasmid, we have discovered that all generated clones have a number of amino acid-changing mutations located in the central region of the gene (Figure S1). To eliminate the possibility that these mutations were the result of our cloning efforts, we have sequenced the host plasmid and the same mutations were discovered. Through discussions with the original research group who donated the plasmid to the Addgene repository, we were told that no mutations were introduced, and that the plasmid contains the wild type sequence of InaZ from *Pseudomonas syringae*. Surprisingly, the last sequence record for InaZ is dated back to 1993 (GenBank: X03035.1) and, despite the extensive interest in this protein, the sequence has not been updated since. Interestingly, the newly-discovered nucleotide mutations in the Addgene plasmid result in amino acid changes that are in better consensus with the rest of the repetitive central region (Figure S1). The latter suggests that the discrepancy is the most likely the result of sequencing errors in early days, arisen from using error-prone PAGE electrophoresis.

Initially, we generated two template plasmids where one contained a full-length InaZ gene and the second had a truncated version with the N-terminal domain removed. The latter InaZ fragment, short of the

first 175 amino acids, will be referred as InaZΔN. Based on early reports, we posited that the N-terminal domain does not play role in the ice nucleation and that its removal could potentially eliminate a hydrophobic domain that might hinder solubility. Both plasmids had a 3xFLAG purification tag positioned on the N-terminal of the gene. During our cell-free expression trials, InaZ and InaZΔN proteins were both expressed in high yield and were found soluble. Unfortunately, we were unable to purify those using a 3xFLAG tag, the procedure that was well optimized in house for many other proteins (data not shown). It is worth noting that the 3xFLAG on InaZ was positioned before the N-terminal domain while the 3xFLAG on InaZΔN sat next to the central domain. However, the 175 amino acid difference in the 3xFLAG position relative to InaZ central region did not have any role on the purification. Based on these observations, we thought that a highly hydrophilic 3XFLAG tag (pI 3.6) might potentially interact with the central domain of InaZ and thus prevent its proper binding to the separation matrix. Thus, we next introduced a more neutral V5 epitope tag (pI 5.71) in both plasmid constructs. Once again, both V5-fused constructs were successfully expressed but the purification procedures failed for both (data not shown). Our next strategy was to re-position the 3xFLAG tag on the C-terminus of the gene and to conduct additional purification trials. The cell-free synthesis using the latter constructs was successful, and both proteins were produced in good yields (Figure 1A, lanes 1-3). The purification procedure was only slightly more efficient where 2.5% of product was recovered for both constructs (Figure 1A, lane 7). Worth to note that both full-length InaZ (123kDa with the tag) and InaZΔN (103 kDa with the tag) displayed retarded mobility on the SDS-PAGE, displaying higher molecular mass of >150 kDa. The same unique behavior of INPs on PAGE has been reported[18,27], suggesting that the cell-free synthesized protein have retained such unique properties.

Despite quite low recovery, the final proteins were of good purity and amounts, suitable for a preliminary structural analysis using Transmission Electron Microscopy in combination with negative staining (Figure 2). As clearly seen from a few select TEM images, both InaZ and InaZΔN proteins lacked any defined oligomeric state. Quite heterogeneous population of complexes, which range from small protein assemblies to higher molecular weight protein aggregates, are clearly observed. Interestingly, a frequent occurrence of rod-like protein organization was manifested in the case of InaZΔN (Figure 2B). No such architectures were found in the full-length InaZ (Figure 2A). One possible explanation is that the presence of a relatively hydrophobic N-terminal domain interfered with the formation of such rod-like assemblies. Interestingly, previous computational modeling studies suggested that 16 amino acid repeats (in the central domain) form loops, which are further organized in β-helix[12,15,28]. This helix is reminiscent of a tube where the dimensions of 2 nm in width and around 30 nm in length would correspond to InaZ monomer. Similar dimensions have been recorded for the rod-like structures observed by TEM. While the fraction of such structures is minor, another possibility is that the absence of cell membrane offers more protein conformational sampling in 3D dimensional space.

Overall, the obtained results on the cell-free expressed InaZ were consistent with previous scientific reports done on native InaZ which suggested a heterogenous multimeric nature for this protein[13,14,16].The high-order of InaZ assembly/organization, where tags are hidden, can also explain why tag-based purification approaches largely failed. In terms of protein yields, based on in-gel quantification of InaZ, 6 ml reaction volume generated 130 μg of protein in the case of InaZ and 144 μg of protein in the case of InaZΔN in the crude translation mixture.

Wheat germ cell-free protein synthesis platforms is an "open-format" system where translation mixture can be also supplemented with liposomes, creating the proper environment for newly synthesized hydrophobic regions of protein and at the same time providing means for protein purification[29]. Due to the presence of hydrophobic N-terminal domain in the full-length InaZ, the protein synthesis was also attempted in the presence of liposomes in the bilayer-dialysis translation format (Figure 1B). This format yielded 375 μg of InaZ (from 2.5 ml reaction volume) where 12% of the protein product (complexed with liposome) were purified from the rest of the crude protein mixture by centrifugation. Such recovery rate can be explained by the lack of defined transmembrane domains in the N-terminal domain and rather weak, possibly transient, interaction with the liposome. As mentioned previously, high order of InaZ assembly

had a possible impact as well. The protein fraction of full-length InaZ with liposome was further designated as InaZ-liposome.

While this work overcame the difficulty in producing full-length and truncated InaZ proteins, we also wanted to confirm that these proteins were still ice nucleation functional. We therefore conducted ice nucleation experiments using dynamic ESEM (Figure 3) to determine the onset of early ice nucleation events or failure to nucleate prior to water saturation. The InaZΔN and InaZ-liposome samples were subjected to this test. ESEM images clearly demonstrated that whenever InaZ protein was present in the sample, ice nucleation event occurred prior to water saturation (Figure 3). At 250 K, the onset of nucleation occurred at 113% relative humidity with respect to ice, RH_{ice}, for InaZΔN and at 109 % RH_{ice} for InaZ-liposome. A slightly better perfomance of InaZ-liposome can be attributed to the higher amounts of InaZ used in the sample. The obtained RHice values for cell-free produced proteins were in exellent agreement with the values previously recorded for SNOMAX, a brand name for P. syringae cells, which were in 110 to 120% range[30]. In addition, based on these results, we confirmed that the N-terminal 175 amino acids do not impact ice nucleation capability even in recombinantly expressed InaZ.

Conclusion

Ice nucleation potentials of bacteria have been studied intensively due to their roles in precipitation and frost injury of plants. Certain bacteria with a membrane bound protein around 120-180kDa in size can nucleate ice at warmer temperature (>263K)[27,31]. The bacterium *Pseudomonas syringae* that possesses InaZ on its outer layer has been utilized and is known as the best ice-inducing agent for decades in the snow-making industry[32]. InaZ protein been just recently demonstrated to perform reliable freeze-thaw valving in the microfluidic devices, providing also a reduction in cost and design complexity of these elements[33]. The successful expression of functional InaZ protein using wheat-germ cell-free platform provides means for generating large volumes of functional InaZ and we expect that other INP proteins can be successfully expressed using the same approach. The flexibility of the cell-free platform also portends the ability to construct and express synthetic InaZ analogs with desired properties in the future. For example, adjusting the number of repeats may allow tuning of freezing conditions or allow the InaZ to improve solubility or limit heterogenous aggregation to permit high-resolution structural studies. Alternatively, rapid cell-free expression in combination with mutational analysis can provide future help in understanding the ice nucleation mechanism as a function of the protein molecular properties. Finally, since we demonstrated that InaZΔN remains functional as full-length protein we could potentially attach other "scaffolds" in place of the N-terminus to create hybrid proteins for a number of applications. For instance, as substitute to tag-based purification, an artificially added multi-pass transmembrane domain could be added to the front of InaZΔN fragment to improve insertion into liposomes or nanodiscs to possibly achieve higher recovery rates and controlled oligomerization. Overall, the successful expression of InaZ in a soluble form using the cell-free platform described here opens many new avenues for potential research on this environmentally and industrially relevant class of proteins.

Acknowledgements: Work was supported by DOE-BER Mesoscale to Molecules Bioimaging Project FWP# 66382. A portion of the research was performed using the Environmental Molecular Sciences Laboratory (EMSL), a national scientific user facility sponsored by the Department of Energy's Office of Biological and Environmental Research and located at PNNL. We thank Dr. Greg Gloor for assistance in the InaZ sequence correction.

Author contributions: JEE managed all aspects of this work. JEE and IVN devised experiments for the study. IVN performed genetics, molecular biology, cell-free expression and negative stain electron microscopy experiments. SC conducted experiments dynamic environmental scanning electron microscopy experiments. All authors contributed to writing the manuscript and approve of the contents.

Conflicts of Interest: The authors declare no competing interests or conflicts of interest.

References

1. Maki, L. R., Galyan, E. L., Chang-Chien, M. M., & Caldwell, D. R. (1974). Ice nucleation induced by pseudomonas syringae. Appl Microbiol, 28(3), 456-459.
2. Lindow, S. E., Arny, D. C., & Upper, C. D. (1978). Distribution of ice nucleation-active bacteria on plants in nature. Appl Environ Microbiol, 36(6), 831-838.
3. Hirano, S. S., Baker, L. S., & Upper, C. D. (1985). Ice nucleation temperature of individual leaves in relation to population sizes of ice nucleation active bacteria and frost injury. Plant Physiol, 77(2), 259-265.
4. Lindow, S. E., Hirano, S. S., Barchet, W. R., Arny, D. C., & Upper, C. D. (1982). Relationship between Ice Nucleation Frequency of Bacteria and Frost Injury. Plant Physiology, 70(4), 1090-1093.
5. Constantinidou, H. A., Hirano, S. S., Baker, L. S., & Upper, C. D. (1990). Atmospheric Dispersal of Ice Nucleation-Active Bacteria - the Role of Rain. Phytopathology, 80(10), 934-937.
6. Attard, E., Yang, H., Delort, A. M., Amato, P., Poschl, U., Glaux, C., . . . Morris, C. E. (2012). Effects of atmospheric conditions on ice nucleation activity of Pseudomonas. Atmospheric Chemistry and Physics, 12(22), 10667-10677.
7. Failor, K. C., Schmale, D. G., Vinatzer, B. A., & Monteil, C. L. (2017). Ice nucleation active bacteria in precipitation are genetically diverse and nucleate ice by employing different mechanisms. Isme Journal, 11(12), 2740-2753.
8. Christner, B. C., Morris, C. E., Foreman, C. M., Cai, R. M., & Sands, D. C. (2008). Ubiquity of biological ice nucleators in snowfall. Science, 319(5867), 1214-1214.
9. Green, R. L., & Warren, G. J. (1985). Physical and Functional Repetition in a Bacterial Ice Nucleation Gene. Nature, 317(6038), 645-648.
10. Li, Q. Q., Yan, Q., Chen, J. S., He, Y., Wang, J., Zhang, H. X., . . . Li, L. (2012). Molecular Characterization of an Ice Nucleation Protein Variant (InaQ) from Pseudomonas syringae and the Analysis of Its Transmembrane Transport Activity in Escherichia coli. International Journal of Biological Sciences, 8(8), 1097-1108.
11. Green, R. L., Corotto, L. V., & Warren, G. J. (1988). Deletion Mutagenesis of the Ice Nucleation Gene from Pseudomonas-Syringae S203. Molecular & General Genetics, 215(1), 165-172.
12. Hudait, A., Odendahl, N., Qiu, Y., Paesani, F., & Molinero, V. (2018). Ice-Nucleating and Antifreeze Proteins Recognize Ice through a Diversity of Anchored Clathrate and Ice-like Motifs. J Am Chem Soc, 140(14), 4905-4912.
13. Govindarajan, A. G., & Lindow, S. E. (1988). Size of bacterial ice-nucleation sites measured in situ by radiation inactivation analysis. Proc Natl Acad Sci U S A, 85(5), 1334-1338.
14. Kajava, A. V., & Lindow, S. E. (1993). A model of the three-dimensional structure of ice nucleation proteins. J Mol Biol, 232(3), 709-717.
15. Garnham, C. P., Campbell, R. L., Walker, V. K., & Davies, P. L. (2011). Novel dimeric beta-helical model of an ice nucleation protein with bridged active sites. Bmc Structural Biology, 11.
16. Ling, M. L., Wex, H., Grawe, S., Jakobsson, J., Londahl, J., Hartmann, S., . . . Santl-Temkiv, T. (2018). Effects of Ice Nucleation Protein Repeat Number and Oligomerization Level on Ice Nucleation Activity. Journal of Geophysical Research-Atmospheres, 123(3), 1802-1810.
17. Watabe, S., Abe, K., Hirata, A., Emori, Y., Watanabe, M., & Arai, S. (1993). Large-Scale Production and Purification of an Erwinia-Ananas Ice Nucleation Protein and Evaluation of Its Ice Nucleation Activity. Bioscience Biotechnology and Biochemistry, 57(4), 603-606.
18. Schmid, D., Pridmore, D., Capitani, G., Battistutta, R., Neeser, J. R., & Jann, A. (1997). Molecular organisation of the ice nucleation protein InaV from Pseudomonas syringae. FEBS Lett, 414(3), 590-594.
19. Han, Y. J., Song, H., Lee, C. W., Ly, N. H., Joo, S. W., Lee, J. H., . . . Park, S. (2017). Biophysical characterization of soluble Pseudomonas syringae ice nucleation protein InaZ fragments. Int J Biol Macromol, 94(Pt A), 634-641.

20. Bassi, A. S., Ding, D. N., Gloor, G. B., & Margaritis, A. (2000). Expression of single chain antibodies (ScFvs) for c-myc oncoprotein in recombinant Escherichia coli membranes by using the ice-nucleation protein of Pseudomonas syringae. Biotechnology Progress, 16(4), 557-563.
21. Wang, B., Knopf, D. A., China, S., Arey, B. W., Harder, T. H., Gilles, M. K., & Laskin, A. (2016). Direct observation of ice nucleation events on individual atmospheric particles. Physical Chemistry Chemical Physics, 18(43), 29721-29731.
22. Wang, B. B., & Knopf, D. A. (2011). Heterogeneous ice nucleation on particles composed of humic-like substances impacted by O-3. Journal of Geophysical Research-Atmospheres, 116.
23. China, S., Alpert, P. A., Zhang, B., Schum, S., Dzepina, K., Wright, K., . . . Knopf, D. A. (2017). Ice cloud formation potential by free tropospheric particles from long-range transport over the Northern Atlantic Ocean. Journal of Geophysical Research-Atmospheres, 122(5), 3065-3079.
24. Murphy, D. M., & Koop, T. (2005). Review of the vapour pressures of ice and supercooled water for atmospheric applications. Quarterly Journal of the Royal Meteorological Society, 131(608), 1539-1565.
25. Sawasaki, T., Hasegawa, Y., Tsuchimochi, M., Kamura, N., Ogasawara, T., Kuroita, T., & Endo, Y. (2002). A bilayer cell-free protein synthesis system for high-throughput screening of gene products. FEBS Lett, 514(1), 102-105.
26. Harbers, M. (2014). Wheat germ systems for cell-free protein expression. FEBS Lett, 588(17), 2762-2773.
27. Wolber, P. K., Deininger, C. A., Southworth, M. W., Vandekerckhove, J., Vanmontagu, M., & Warren, G. J. (1986). Identification and Purification of a Bacterial Ice-Nucleation Protein. Proc Natl Acad Sci U S A, 83(19), 7256-7260.
28. Graether, S. P., & Jia, Z. (2001). Modeling Pseudomonas syringae ice-nucleation protein as a beta-helical protein. Biophys J, 80(3), 1169-1173.
29. Nozawa, A., Nanamiya, H., Miyata, T., Linka, N., Endo, Y., Weber, A. P. M., & Tozawa, Y. (2007). A cell-free translation and proteoliposome reconstitution system for functional analysis of plant solute transporters. Plant and Cell Physiology, 48(12), 1815-1820.
30. Chernoff, D. I., & Bertram, A. K. (2010). Effects of sulfate coatings on the ice nucleation properties of a biological ice nucleus and several types of minerals. Journal of Geophysical Research-Atmospheres, 115.
31. Lindow, S. E., Lahue, E., Govindarajan, A. G., Panopoulos, N. J., & Gies, D. (1989). Localization of Ice Nucleation Activity and the Icec Gene-Product in Pseudomonas-Syringae and Escherichia-Coli. Molecular Plant-Microbe Interactions, 2(5), 262-272.
32. Cochet, N., & Widehem, P. (2000). Ice crystallization by Pseudomonas syringae. Appl Microbiol Biotechnol, 54(2), 153-161.
33. Gaiteri, J. C., Henley, W. H., Siegfried, N. A., Linz, T. H., & Ramsey, J. M. (2017). Use of Ice-Nucleating Proteins To Improve the Performance of Freeze-Thaw Valves in Microfluidic Devices. Analytical Chemistry, 89(11), 5999-6006.

Figures and Figure Captions

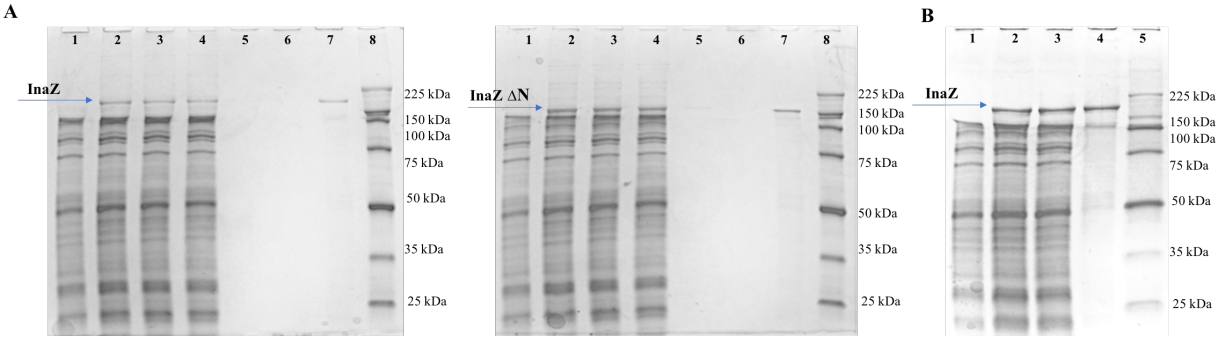

Figure1. Cell-free synthesis and purification of InaZ proteins. A. SDS-PAGE gels showing expression and purification of InaZ (on the left) and InaZΔN (on the right) using a standard bilayer format. Lane 1, control expression with no plasmid (negative control); Lane 2, crude mixture; Lane 3, soluble fraction; Lane 4, flow-through; Lane 5, elution fraction 1; Lane 6, elution fraction 2; Lane 7, elution fractions 1 and 2 combined and concentrated; Lane 8, MW markers. B. SDS-PAGE gels showing expression and purification of InaZ where the translation mixture was supplemented with liposomes (a bilayer+dialysis format). Lane 1, control expression with no plasmid; Lane 2, crude mixture; Lane 3, supernatant (or flow-through); Lane 4, re-suspended pellet (final product); Lane 5, MW markers.

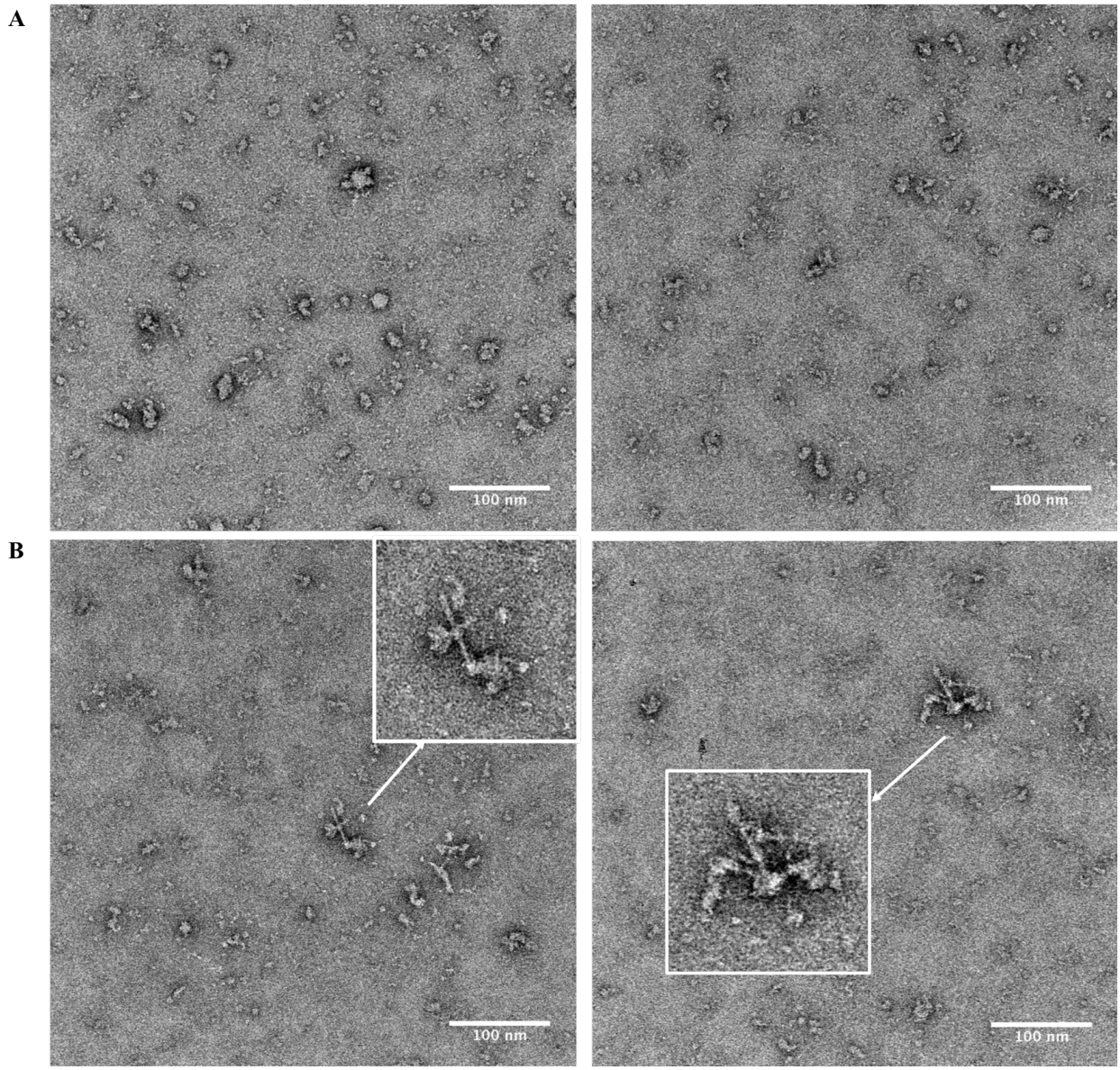

Figure 2. TEM characterization of InaZ proteins. A. TEM images of negatively stained full-length InaZ. B. TEM images of negatively stained InaZΔN. The zoom-in images of rod-like structures are denoted with white arrows.

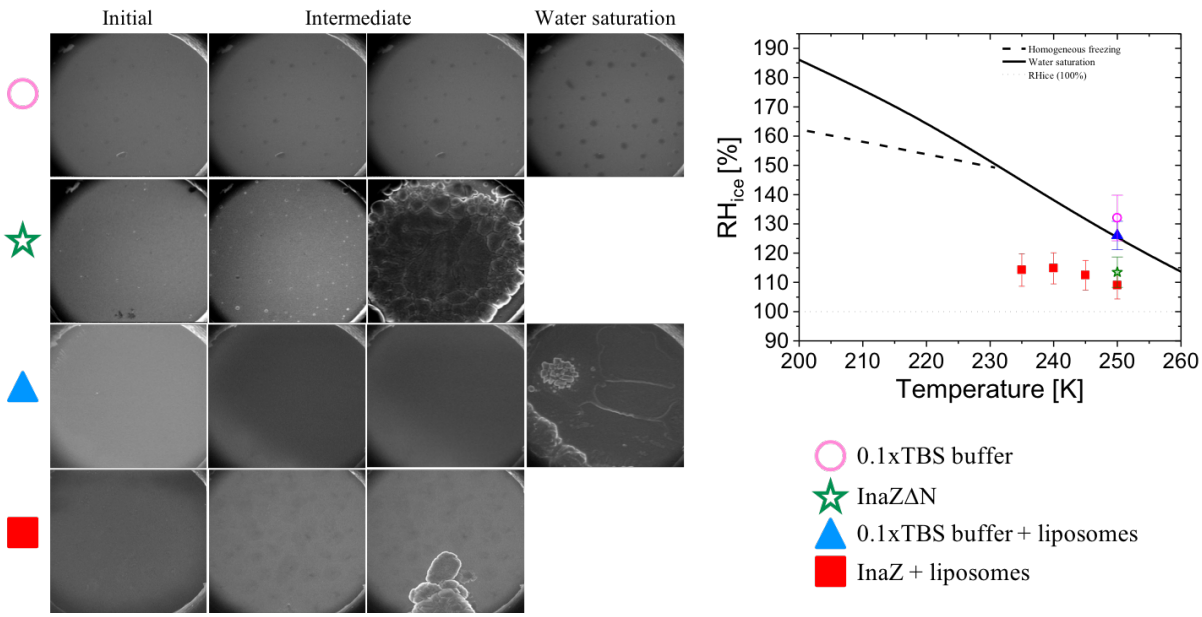

Figure 3. Monitoring ice formation on the sample droplets using dynamic ESEM. Recorded ESEM images (on the left) show initial, intermediate and water saturation conditions. The white scale bar corresponds to 100 microns. The mean relative humidity with respect to ice (RH_{ice}) for the nucleation event has been calculated (on the right). Droplets from InaZ-liposome samples were investigated at multiple temperatures to derive RH_{ice}. The error bars were derived from experimental uncertainties.